CrossMark

Carnosine modulates nitric oxide in stimulated murine RAW 264.7 macrophages

Giuseppe Caruso[1,2] · Claudia G. Fresta[1,2] · Francisco Martinez-Becerra[2,3] · Lopalco Antonio[2] · Ryan T. Johnson[4] · Richard P. S. de Campos[1,2,5] · Joseph M. Siegel[1,2] · Manjula B. Wijesinghe[1,2] · Giuseppe Lazzarino[6] · Susan M. Lunte[1,2,4]

Abstract Excess nitric oxide (NO) production occurs in several pathological states, including neurodegeneration, ischemia, and inflammation, and is generally accompanied by increased oxidative/nitrosative stress. Carnosine [β-alanine-histidine (β-Ala-His)] has been reported to decrease oxidative/nitrosative stress-associated cell damage by reducing the amount of NO produced. In this study, we evaluated the effect of carnosine on NO production by murine RAW 264.7 macrophages stimulated with lipopolysaccharides + interferon-γ. Intracellular NO and intracellular and extracellular nitrite were measured by microchip electrophoresis with laser-induced fluorescence and by the Griess assay, respectively. Results showed that carnosine causes an apparent suppression of total NO production by stimulated macrophages accompanied by an unexpected simultaneous drastic increase in its intracellular low toxicity endproduct, nitrite, with no inhibition of inducible nitric oxide synthase (iNOS). ESI-MS and NMR spectroscopy in a cell-free system showed the formation of multiple adducts (at different ratios) of carnosine-NO and carnosine-nitrite, involving both constituent amino acids (β-Ala and His) of carnosine, thus providing a possible mechanism for the changes in free NO and nitrite in the presence of carnosine. In stimulated macrophages, the addition of carnosine was also characterized by changes in the expression of macrophage activation markers and a decrease in the release of IL-6, suggesting that carnosine might alter M1/M2 macrophage ratio. These results provide evidence for previously unknown properties of carnosine that modulate the NO/nitrite ratio of stimulated macrophages. This modulation is also accompanied by changes in the release of pro-inflammatory molecules, and does not involve the inhibition of iNOS activity.

Keywords Nitric oxide · Nitrite · Carnosine · Microchip electrophoresis · Macrophages · Cytokines secretion

Ryan T. Johnson, Richard P. S. de Campos, Joseph M. Siegel and Manjula B. Wijesinghe have contributed equally to this work.

Electronic supplementary material The online version of this article (doi:10.1007/s11010-017-2991-3) contains supplementary material, which is available to authorized users.

✉ Giuseppe Lazzarino
lazzarig@unict.it

✉ Susan M. Lunte
slunte@ku.edu

1   Ralph N. Adams Institute for Bioanalytical Chemistry, University of Kansas, Lawrence, KS, USA

2   Department of Pharmaceutical Chemistry, University of Kansas, Lawrence, KS, USA

3   Immunology Core Laboratory of the Kansas Vaccine Institute, University of Kansas, Lawrence, KS, USA

4   Department of Chemistry, University of Kansas, Lawrence, KS, USA

5   Department of Chemistry, State University of Campinas, Campinas, Brazil

6   Division of Medical Biochemistry, Department of Biomedical and Biotechnological Sciences, University of Catania, Catania, Italy

Abbreviations

Arg	L-Arginine
β-Ala	β-Alanine
BSA	Bovine serum albumin
Car	Carnosine
Cit	L-Citrulline
CD86	Cluster of differentiation 86
CD206	Cluster of differentiation 206
CID	Collision-induced dissociation

DAF-FM DA	4-Amino-5-methylamino-2′,7′-difluorofluorescein diacetate
DEA/NO	Diethylammonium (Z)-1-(N,N-diethyl-amino)diazen-1-ium-1,2-diolate
DMEM	Dulbecco's modified Eagle's medium
DMSO	Dimethyl sulfoxide
ESI-MS	Electrospray mass spectrometry
FBS	Fetal bovine serum
FMO	Fluorescence minus one
His	L-Histidine
IFN-γ	Interferon-γ
IL-1β	Interleukin-1β
IL-2	Interleukin-2
IL-4	Interleukin-4
IL-5	Interleukin-5
IL-6	Interleukin-6
IL-10	Interleukin-10
IL-12	Interleukin-12
iNOS	Inducible nitric oxide synthase
KC	Keratinocyte chemoattractant
LPS	Lipopolysaccharides
ME-LIF	Microchip electrophoresis with laser-induced fluorescence
MHCII	Major histocompatibility complex class II
NMR	Nuclear magnetic resonance
NO	Nitric oxide
NO_2^-	Nitrite
PBS	Phosphate-buffered saline
PDMS	Polydimethylsiloxane
RNS	Reactive nitrogen species
ROS	Reactive oxygen species
SDS	Sodium dodecyl sulfate
TNF-α	Tumor necrosis factor α

Introduction

Nitric oxide (NO) is an important gaseous molecule that transmits both intracellular and intercellular signals crucial for cell survival [1]. Physiologically, NO is the most important vasodilator and regulator of the vascular tone and blood flow [2] and is involved in several additional processes, including platelet aggregation, neurotransmission, and the immune response [3]. During its 3–6 s half-life in vivo, NO can diffuse relatively long distances in the extracellular space (across membranes) and interact with neighboring cells [4]. NO is generated in cells by a group of enzymes known as nitric oxide synthase (NOS), which generate NO through the conversion of L-arginine (Arg) to L-citrulline (Cit) [5]. It is well known that there are three major NOS isoforms: endothelial NOS (eNOS), neuronal NOS (nNOS), and inducible NOS (iNOS). While nNOS and eNOS are constitutively expressed, iNOS, which is

found primarily in glia and macrophages, is overexpressed under a variety of acute and chronic pathological conditions [6] and is a part of the immune response following tissue injury or inflammation [7].

In the immune system, macrophages are the primary cell type that is activated [8], usually producing NO through the overexpression of iNOS. Uncontrolled cellular production of NO by macrophages is generally coupled to increased production of reactive oxygen species (ROS). ROS, such as superoxide, can react with NO to generate highly reactive nitrogen species (RNS) such as peroxynitrite. The interaction of ROS and RNS with important biological molecules (proteins, nucleic acids, membrane lipids) can irreversibly alter their functions and lead to cell death [9]. This oxidative/nitrosative stress pathway has been implicated in many neurodegenerative, cardiovascular, and systemic disorders [10]. To mitigate the damaging effects of ROS and RNS, it is essential for the cell to maintain an appropriate level of low molecular weight antioxidants [11–14].

Carnosine (Car) is a naturally occurring endogenous imidazole dipeptide [β-alanine-histidine (β-Ala-His)] that is synthesized from its component amino acids by the enzyme Car synthase. Car is widely distributed in animal tissues, with the highest concentrations observed in brain and in cardiac and skeletal muscle (up to 20 mM) [15]. There are many reports in the literature stating that Car plays an important role in various physiological cell functions in vertebrates, including humans. For instance, it has been reported that Car is involved in many processes of cellular defense, including inhibition of protein crosslinking and ROS and RNS detoxification [16, 17]. In addition, the imidazole ring of the His residue in Car is capable of chelating transition metal ions, especially Cu(II) and Zn(II) [18]. Car has also been reported to reduce peroxynitrite-dependent tyrosine nitration of proteins [19], possibly by acting as a direct NO trapper [20]. The protective effects of Car with regard to both ROS and RNS toxicity make it a putative candidate for an effective pharmacological antioxidant therapy [21]. Notwithstanding the abundant literature on Car, little is known about the effects of this endogenous dipeptide on macrophages stimulated to overproduce NO as part of the immune response. In addition, the mechanism of action through which Car decreases NO toxicity both in vitro and in vivo is still under debate.

It is still not known whether Car modulates activation markers and cytokines secretion of polarized M1 (pro-inflammatory) macrophages. While M1 macrophages are activated by stimulation with interferon-γ (IFN-γ) and/or lipopolysaccharides (LPS), M2 macrophages are generated after stimulation with interleukin (IL)-4 and IL-13, and are mainly characterized by expression of CD206 (mannose receptor) [22]. While M1 macrophages are more efficient at producing NO, M2 macrophages [23] tend toward

ornithine production, through the expression of arginase I. This enzyme utilizes Arg that would otherwise be employed by iNOS to produce NO [24] and instead generates ornithine and L-proline among other products [25]. It has been demonstrated that the production of ROS is essential for both M1 antimicrobial activity and generation of M2 polarized macrophages [26].

In this study, the effects of Car on stimulated murine RAW 264.7 macrophages were investigated by measuring NO, nitrite, and iNOS activity. The expression of macrophage activation markers and cytokine release connected to Car modulation of NO was also probed, with the aim of improving our knowledge of Car mechanisms in this cell system.

Materials and methods

Materials and reagents

Murine RAW 264.7 cells (ATCC® TIB71™), Dulbecco's Modified Eagle's Medium (DMEM), phenol red-free DMEM, fetal bovine serum (FBS), and penicillin/streptomycin antibiotic solution were purchased from American Type Culture Collection (ATCC, Manassas, VA, USA). L-Carnosine (Car), L-histidine (His), β-alanine (β-Ala), Griess reagent (modified), anhydrous dimethyl sulfoxide (DMSO), phosphate-buffered saline (PBS), monobasic and dibasic phosphate, trypan blue solution, lipopolysaccharides (LPS) from *E. coli* 0111:B4, bovine serum albumin (BSA), sodium nitrite, tetradeuteromethanol (CD₃OD, ≥99.8 atom % D), and sodium dodecyl sulfate (SDS) were all supplied by Sigma-Aldrich (St. Louis, MO, USA). 4-Amino-5-methylamino-2′,7′-difluorofluorescein diacetate (DAF-FM DA) was purchased from Invitrogen (Carlsbad, CA, USA). Boric acid, sodium hydroxide, acetone, 2-propanol (IPA), and ethanol (95%) were obtained from Fisher Scientific (Pittsburgh, PA, USA). Interferon-γ (IFN-γ), mouse, recombinant, *E. coli* was supplied by Calbiochem (Gibbstown, NJ, USA). Polyethersulfone (PES) membrane (3 K) was purchased from VWR International (West Chester, PA, USA). C-Chip disposable hemocytometer was purchased from Bulldog Bio, Inc. (Portsmouth, NH, USA). Diethylammonium (Z)-1-(*N,N*-diethylamino) diazen-1-ium-1,2-diolate (DEA/NO) salt was purchased from Cayman Chemical (Ann Arbor, MI, USA) and stored at −80 °C for no longer than 6 months. Sylgard 184 polydimethylsiloxane (PDMS) prepolymer and curing agent were obtained from Ellsworth Adhesives (Germantown, WI, USA). FC-R blocking antibodies, anti-MHCII, and anti-CD86 were purchased from Tonbo Biosciences (San Diego, CA, USA), anti-CD206 was purchased from Biolegend (San Diego, CA, USA), while Fluorescence Minus One (FMO) was obtained from BD Biosciences (San Jose, CA, USA). Mouse iNOS ELISA Kit was purchased from LSBio (Seattle, WA, USA). All water used was Ultrapure (18.3 MΩ cm) (Milli-Q Synthesis A10, Millipore, Burlington, MA, USA).

Cell culture and treatment protocol

RAW 264.7 macrophage cells were cultured in DMEM containing 10% (v/v) FBS, L-glutamine (2 mM), penicillin (50 IU/mL), and streptomycin (0.3 mg/mL). The cells were cultured in 25 cm² polystyrene culture flasks at a density of 2×10^6 cells/flask, maintained in a humidified environment at 37 °C and 5% CO₂, and passaged every 2 days at about 80–85% confluence to avoid overgrowth.

On the day of the experiment, once the cells adhered to the flask surface, they were pretreated with Car (5, 10, or 20 mM final concentration), β-Ala, His or a combination of β-Ala and His (20 mM final concentration) for 1 h prior to stimulation with 100 ng/mL LPS in combination with 600 U/mL INF-γ. Cells were then incubated for 24 h (to ensure the maximal iNOS activation [20]) in a humidified environment at 37 °C and 5% CO₂. Resting untreated cells were used as a control. At the end of incubation, to analyze intracellular NO production, the cells were washed with cold 10 mM PBS at pH 7.4 and then cultured with phenol red-free DMEM containing DAF-FM DA dye for 50 min. Once inside the cell, the hydrolyzed dye reacts with a partially oxidized species of NO (N₂O₃) to form a stable triazole (DAF-FM T), which has a high fluorescence yield. A stock dye solution of 5 mM DAF-FM DA was prepared in 99% sterile DMSO. Next, 10 µL of this solution (10 µM DAF-FM DA final concentration) was added to each culture flask and allowed to react for 50 min in a humidified environment and 5% CO₂. Cells were then washed again with cold 10 mM PBS at pH 7.4 and incubated in phenol red-free DMEM for an additional 20 min at 37 °C and 5% CO₂. Cells were then harvested using a cell scraper, and 100 µL of the cell suspension was removed for cell counting before centrifuging the suspension at 1.137×*g* for 3 min at 4 °C. The supernatant was removed, and the cell pellet was washed twice with large volumes of cold 10 mM PBS at pH 7.4. Cells were lysed using 300 µL of 10 mM boric acid and 7.5 mM SDS at pH 9.2. The lysate solution was filtered by centrifugation at 18.690×*g* for 6 min at 4 °C in centrifuge tubes equipped with 3 kDa molecular weight cut-off filters. The filtered lysates were then analyzed using the microfluidic device to quantitate intracellular NO concentration [27], while the stable NO endproduct, nitrite, was measured using the Griess assay.

Cell density and viability were measured using a hemocytometer and trypan blue exclusion assay, respectively. The cell suspension was diluted in the ratio of 1:1,

1:2, or 1:3 (based on cell density) with 0.4% trypan blue solution. The number of viable cells and the cell density were determined in each sample using a 4 mm^2 total area C-Chip disposable hemocytometer.

NO detection using microchip electrophoresis with laser-induced fluorescence (ME-LIF)

The fabrication of hybrid PDMS-glass microfluidic devices to carry out the ME-LIF experiments has been described previously [27]. Prior to performing the analysis, the microfluidic device was flushed with 0.1 M NaOH for 5 min, followed by a 5-min flush with run buffer consisting of 10 mM boric acid and 7.5 mM SDS at pH 9.2. Separations were performed in the normal polarity mode using a 30 kV high-voltage power supply (Ultravolt, Ronkonkoma, NY, USA). For all separations, +2400 and +2200 V were applied to the running buffer and sampling reservoirs, respectively. A 1-s gated injection was used to introduce the sample into the separation channel. The system was flushed for 45 s with run buffer after each sample was analyzed.

A Nikon Eclipse Ti-U inverted microscope (Nikon Instruments Inc., Melville, NY, USA) fitted with a 488-nm laser (diode laser, Spectra-Physics, Irvine, CA, USA) was used for excitation, and a photomultiplier tube (Hammatsu Corporation, Bridgewater, NJ, USA) was used for detection. The signal was amplified using a SR570 low-noise current preamplifier at 1 μAV^{-1} (Stanford Research Systems, Sunnyvale, CA, USA). Data acquisition was carried out using a D/A converter (National Instruments, Austin, TX, USA) and an in-house written LabVIEW program. Data analysis was performed using Origin 8.1 software (OriginLab, Northampton, MA, USA). For quantitation of NO in cell lysates, a calibration curve for NO from 0.125 to 4 μM was prepared using the NO-donor DEA/NO as described by Mainz et al. [27].

Nitrite determination using the Griess assay

The Griess assay was performed using 96-well plates and a plate reader (Molecular Devices, Spectra Max M5, Sunnyvale, CA, USA). For extracellular nitrite quantification, 100 μL of supernatant was taken from each flask and added to 100 μL of Griess reagent; for intracellular quantification, 100 μL of Griess reagent was added to 100 μL of filtered cell lysate. After 15 min at room temperature in the dark, the absorbance was measured at 540 nm.

A nitrite standard calibration curve was prepared using nitrite standards from 1 to 100 μM.

Quantification of iNOS

Quantification of iNOS by ELISA was carried out in resting macrophages, macrophages stimulated with LPS + IFN-γ (24 h), and macrophages stimulated with LPS + IFN-γ (24 h) supplemented with 20 mM Car (1 h pretreatment), according to manufacturer's instructions. Macrophage cells were harvested using a cell scraper and centrifuged at 1.137×g for 3 min at 4 °C. The supernatant was removed, and the cell pellet was washed three times using cold 10 mM PBS at pH 7.4 and then resuspended in PBS. Cells were lysed by ultrasonication (four times). After centrifuging at 1500×g for 10 min at 4 °C to remove cellular debris, the supernatant was collected for assaying. One hundred microliters of standard, blank, or sample was added to each well of a 96-well plate, and the plate was covered with a plate sealer and incubated for 2 h at 37 °C. After the incubation step, the liquid was aspirated, and 100 μL of biotin-conjugated detection antibody was added to the wells. The plates were then covered with a plate sealer and incubated (1 h at 37 °C) under gentle agitation to ensure thorough mixing. Unbound detection antibody was washed away using 400 μL of wash buffer (three times). One hundred microliters of avidin-horseradish peroxidase (HRP) conjugate was then added to each well, and the plate was covered with a new plate sealer and incubated (1 h at 37 °C). Unbound Avidin-HRP conjugate was washed away using 400 μL of wash buffer (five times). Next, 90 μL of TMB substrate solution was added to each well, and the plate was covered with a new plate sealer and was incubated for 30 min at 37 °C. Finally, the reaction was terminated by adding 50 μL of stop solution to each well. Absorbance values were measured at 450 nm using a microplate reader. The absorbance of each sample was then compared with a standard curve generated using known antigen concentrations (0–20 ng/mL) in order to determine antigen concentrations.

To further corroborate the immunochemical data, measurement of the Arg/Cit ratio in cell lysates was also performed. Analysis of aliquots of deproteinized cell lysates (25 μL) of resting macrophages, macrophages stimulated with LPS + IFN-γ (24 h), and macrophages stimulated with LPS + IFN-γ (24 h) supplemented with 20 mM Car (1 h pretreatment) were subjected to amino acid analysis. Arg and Cit in the cell lysates were determined following precolumn derivatization with ortho-phthaldialdehyde and 3-mercaptopropionic acid and separation using liquid chromatography (HPLC) with fluorescence detection, as described elsewhere [28].

Electrospray mass spectrometry (ESI-MS) analysis

Samples were prepared by dissolving Car in Milli-Q water in the presence of DEA/NO at a peptide/NO-donor ratio of 1:1. Samples were incubated for 30 min at room temperature. The final Car/DEA/NO (50 μM) solution, consisting of 90/10 Milli-Q water/methanol with 0.4% formic acid, was analyzed by ESI-MS. ESI-MS spectra were recorded on a Thermo LTQ XL linear ion trap mass spectrometer (Waltham, MA, USA). The samples were infused into the ESI source at 10 μL/min using a 500 μL syringe. The spectra were collected in positive ion mode with a spray voltage of 3.5 kV, a cone voltage of 15 V, a tube lens voltage of 40 V, and a capillary temperature of 300 °C. Fragmentation studies were conducted using 15–25 collision-induced dissociation (CID) energy.

Nuclear magnetic resonance (NMR) spectroscopy

The concentrations were 50 mM for both Car and DEA/NO used in the NMR studies. The final volume of the sample was 0.5 mL, and the solvent was 9:1 (v/v) $H_2O:CD_3OD$. All spectra were acquired using 5 mm NMR tubes. 1D ^{13}C-NMR spectra of the dipeptide, the donor, and a mixture of these two compounds were acquired on a 500 MHz Bruker spectrometer (Rheinstetten, Germany) equipped with a carbon-enabled cryoprobe. Sample temperature was set to 25 °C. Data were processed using the software MestreNova (MestreLab Researcher, S. L., Santiago de Compostela, Spain). Chemical shifts for the 1D ^{13}C-NMR spectra were referenced to the signal of CD_3OD.

Cell imaging

Images of morphological changes of the macrophages due to different stimulation protocols were obtained using an Accu-Scope microscope (Mel Sobel Microscopes Ltd, Hicksville, NY, USA) equipped with MicroPublisher 3.3 RTV camera (Qimaging, Surrey, BC, Canada). Image analysis was performed using QCapture Pro 6 software (Qimaging).

Flow cytometry

Following different stimulation protocols (no treatment, LPS + IFN-γ stimulation, in the presence or absence of Car), macrophages were collected and washed using cold 10 mM PBS. After incubating with FC-R blocking antibodies, cells were stained using antibodies against MHCII, CD86, and CD206 in PBS 2% BSA. FMO controls were used to set negative gates for each fluorophore. Cells were then analyzed using a FACSaria Fusion (BD Biosciences, San Jose, CA, USA). Analysis of levels of activation markers was performed using Flowjo 10.1 software (Flowjo, Ashland, OR, USA). Mean fluorescence intensities or percent positive values were analyzed using a one-way ANOVA (for individual markers) or a two-way ANOVA (for M1-M2 activation analysis) using Graphpad (Graphpad software, San Diego, CA, USA).

Cytokine secretion

Supernatants from resting macrophages, macrophages stimulated with LPS + IFN-γ (24 h), and macrophages stimulated with LPS + IFN-γ (24 h) supplemented with 20 mM carnosine (Car) (1 h pretreatment) were collected after cell centrifugation. Samples (25 μL per condition) were then analyzed in triplicate using a U-plex cytokine panel (Meso Scale Discovery, Rockville, MD, USA) containing IFN-γ, IL-1β, IL-2, IL-4, IL-5, IL-6, IL-10, IL12p40, KC, and TNF-α on a 10 spot-96-well plate. The chemiluminescence was measured for each sample/cytokine combination using a Quickplex SQ 120 plate reader (Meso Scale Discovery). The amount of signal was then used to calculate the concentration of each cytokine using a five-parameter logistic fit calculated using a serial dilution of a mixture of calibrated standards of each cytokine. Results were then analyzed using a two-way ANOVA followed by a Tukey test for multiple comparisons (GraphPad).

Statistical analysis

All statistical analyses in this work were performed as follows unless specified otherwise. Normal data distribution was determined using the Kolmogorov–Smirnov test. The within-group comparison was performed by one-way analysis of variance (ANOVA). Differences across groups were estimated by two-way ANOVA. Fisher's protected least square was used as the post hoc test. Only two-tailed p values less than 0.05 were considered statistically significant.

Electronic supplementary material

Online Resource 1 shows the effect of different Car concentrations on intracellular NO in stimulated macrophages. Online Resource 2 depicts the effect of different Car concentrations on intracellular and extracellular nitrite in stimulated macrophages. The effects of the different stimulation protocols on the cell morphology are shown in Online Resource 3. Online Resource 4 and Online Resource 5 report the cell sizes and levels of CD86 in resting and stimulated macrophages (in the presence or absence of Car). Online Resource 6 shows the effect of increasing concentrations of Car on the production of TNF-α in stimulated macrophages.

Results

Effect of Car on NO and nitrite production by stimulated murine macrophage cells

Figure 1a shows the effect of LPS + IFN-γ stimulation on intracellular NO production (as determined by ME-LIF) in cultured macrophages. Stimulation of the cells for 24 h caused an increase in NO production from 0.07 ± 0.02 nmol/10^6 cells in resting macrophages to 2.82 ± 0.32 nmol/10^6 cells ($p < 0.001$ compared to resting cells). The addition of 20 mM Car for 24 h to resting macrophages did not cause any significant change in the basal macrophage NO production (data not shown)

To test the effect of the addition of Car on NO production in stimulated macrophages, 20 mM Car was added 1 h prior to the addition of LPS + IFN-γ. The amount of NO production in this case was much lower than that in the stimulated cells ($p < 0.001$ compared with LPS + IFN-γ treated cells), and it was essentially the same as in untreated resting macrophage cells (0.10 ± 0.01 nmol/10^6 cells) (Fig. 1a). This suggests a potent inhibitory effect of Car on NO production. Figure 1b shows three representative electropherograms obtained for resting (control) cells and cells stimulated in the absence or presence of 20 mM Car (1 h pretreatment). The decrease in NO production by stimulated macrophages in the presence of Car compared

with cells stimulated in the absence of Car can be seen. Online Resource 1 shows the dose-dependent decrease in NO formation induced by increasing Car concentrations in stimulated macrophages.

The intracellular and extracellular concentrations of nitrite, the major metabolite of NO, were measured for the same cell samples using the Griess reaction. For resting cells, the intracellular nitrite concentration was determined to be 0.70 ± 0.15 nmol/10^6 cells (Fig. 2). The addition of Car for 24 h to resting macrophages did not cause any significant change in the basal macrophage nitrite production (data not shown). As expected, following the 24-h challenge with LPS + IFN-γ, the intracellular nitrite production increased to 4.31 ± 0.36 nmol/10^6 cells ($p < 0.001$ compared with resting cells) (Fig. 2). Surprisingly, however, stimulation in the presence of Car (1 h pretreatment) generated a strong increase in intracellular nitrite (8.80 ± 0.75 nmol/10^6 cells), approximately two times higher than that in cells stimulated with LPS + IFN-γ alone (2.04 times higher, $p < 0.001$). Mean values of intracellular nitrite 12.6 times higher than that of untreated cells (control) ($p < 0.001$) were determined for stimulated cells in the presence of Car.

The measurement of extracellular nitrite production in cell medium (Fig. 2) shows that stimulation with LPS + IFN-γ caused an increase in nitrite from 0.65 ± 0.16 nmol/10^6 cells for resting macrophages to 5.26 ± 0.42 nmol/10^6 cells ($p < 0.001$). In samples
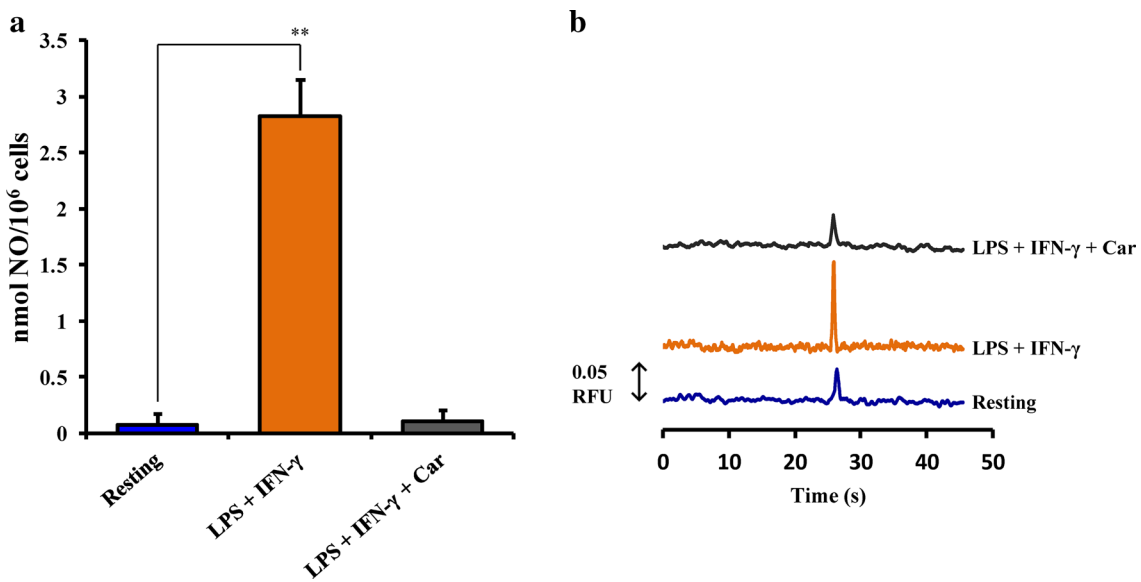

Fig. 1 Intracellular concentrations of NO (as detected by microchip electrophoresis with laser-induced fluorescence) in resting macrophages, in macrophages stimulated with LPS + IFN-γ (24 h), and in macrophages stimulated with LPS + IFN-γ (24 h) supplemented with 20 mM carnosine (Car) (1 h pre-treatment) (**a**). Representative electropherograms showing the change in the height of the NO peak in the cell lysates of resting macrophages, of macrophages stimulated

with LPS + IFN-γ (24 h), and of macrophages stimulated with LPS + IFN- γ (24 h) supplemented with 20 mM car (1 h pre-treatment) (**b**). Values are the mean of five different experiments. *Vertical bars* represent standard deviations. Significant comparisons between each group are indicated by *lines*. **Significantly different from resting (p < 0.001)
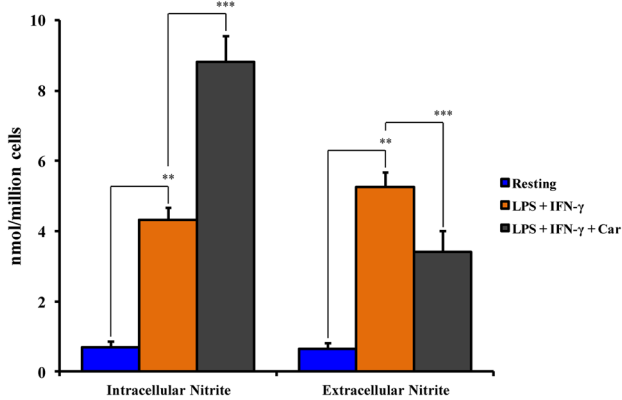
Fig. 2 Intracellular and extracellular concentrations of nitrite in resting macrophages, in macrophages stimulated with LPS + IFN-γ (24 h), and in macrophages stimulated with LPS + IFN-γ (24 h) supplemented with 20 mM carnosine (Car) (1 h pretreatment). Values are the mean of five different experiments. Standard deviations are represented by *vertical bars*. Significant comparisons between each group are indicated by *lines*. **Significantly different from resting ($p < 0.001$); ***significantly different from LPS + IFN-γ ($p < 0.001$)

Table 1 Arg/Cit ratio variation as an indicator of iNOS activity

Cell treatment	Arg/Cit ratio
Resting	2.13 ± 0.57
LPS + IFN-γ	0.23 ± 0.21
LPS + IFN-γ + Car	0.21 ± 0.10

Arg/Cit ratio (as determined by HPLC with fluorescence detection) in resting macrophages, in macrophages stimulated with LPS + IFN-γ (24 h), and in macrophages stimulated with LPS + IFN-γ (24 h) supplemented with 20 mM carnosine (Car) (1 h pretreatment). Values are the mean of three different experiments $\pm$ SD

pretreated with Car, a moderate increase in extracellular nitrite formation in stimulated macrophages was observed ($3.41 \pm$ nmol/10^6 cells, $p < 0.001$ compared with both resting and LPS + IFN-γ stimulated macrophages). The effect of increasing Car concentration (5–20 mM) on intracellular and extracellular nitrite formation is shown in Online Resource 2.

To investigate the observed effect on nitrite production by murine macrophages in the presence of Car, we performed additional experiments in which intracellular and extracellular nitrite were measured after incubating the cells for 24 h with LPS + IFN-γ following a 1 h preincubation with β-Ala, His, or β-Ala + His (all at 20 mM). In stimulated macrophages, neither β-Ala nor His nor their equimolar combination induced significant changes in intracellular and extracellular nitrite compared with macrophages stimulated with LPS + IFN-γ (data not shown).

Evaluation of iNOS protein expression in macrophage cell lysates

iNOS expression in different cell samples (no treatment, LPS + IFN-γ stimulation, in the presence or absence of Car) was measured immunoenzymatically by ELISA. As expected, resting macrophages did not express a measurable amount of iNOS. When challenged for 24 h with LPS + IFN-γ, iNOS expression was easily quantified, and this level was then set as the maximum level of iNOS protein expression (100% iNOS). Cells pretreated with Car (1 h) before stimulation with LPS + IFN-γ did not show significant decrease in iNOS protein expression

($92.12 \pm 6.47\%$) compared with cells stimulated in the absence of Car.

To verify the ELISA results, we carried out an indirect measurement of iNOS following treatments with LPS + IFN-γ (24 h), without and with 20 mM Car (1 h pretreatment). This was accomplished by measuring the concentrations of Arg and Cit in cell lysates. The Arg/Cit ratio, directly connected to the production of NO [5], was then used as an indicator of total NOS activity. As shown in Table 1, the Arg/Cit ratio in resting macrophages was equal to 2.13 ± 0.57. In stimulated macrophages, without and with Car, these ratios were 0.23 ± 0.21 and 0.21 ± 0.10, respectively ($p < 0.001$ compared with resting cells). Hence, cells stimulated by LPS + IFN-γ in both the presence and the absence of Car had 9- and 10.1-fold increases in total NOS activity, respectively. It can therefore be concluded that Car did not inhibit LPS + IFN-γ-induced activity of iNOS. This increase in NOS activity can fully be attributed to iNOS, since this is the only inducible form of NOS [29].

ESI-MS analysis to study the interaction mechanism of Car with NO

ESI-MS^n measurements were carried out with the intent to better understand the interaction that occurs between Car and NO. In 1:1 Car:NO-donor (DEA/NO) solution, two peaks attributable to Car–NO adducts were observed at m/z 287 [Car + 2NO]H$^+$ and m/z 304 [Car + NO + NO$_2$] H$^+$, with the first adduct having a higher intensity (Fig. 3a). A peak at m/z 567, attributed to the formation of Car–dimer–NO adducts, [2Car + 2NO$_2$]Na$^+$ or [2Car + NO + NO$_2$]K$^+$, was also detected (Fig. 3b). The CID products of the peak at 567 m/z led to the formation of additional degradation products and [Car]H$^+$ (data not shown). Figure 3c shows the fragmentation profile obtained from m/z 287, where the most prominent peaks are represented by m/z 269 [Car + 2NO – H$_2$O]H$^+$, m/z 241 [Car + 2NO – H$_2$O – CO]H$^+$, and m/z 177. Three peaks corresponding to m/z ratios of 286 [Car + NO + NO$_2$ – H$_2$O] H$^+$, 258 [Car + NO + NO$_2$ – H$_2$O – CO]H$^+$, and 212
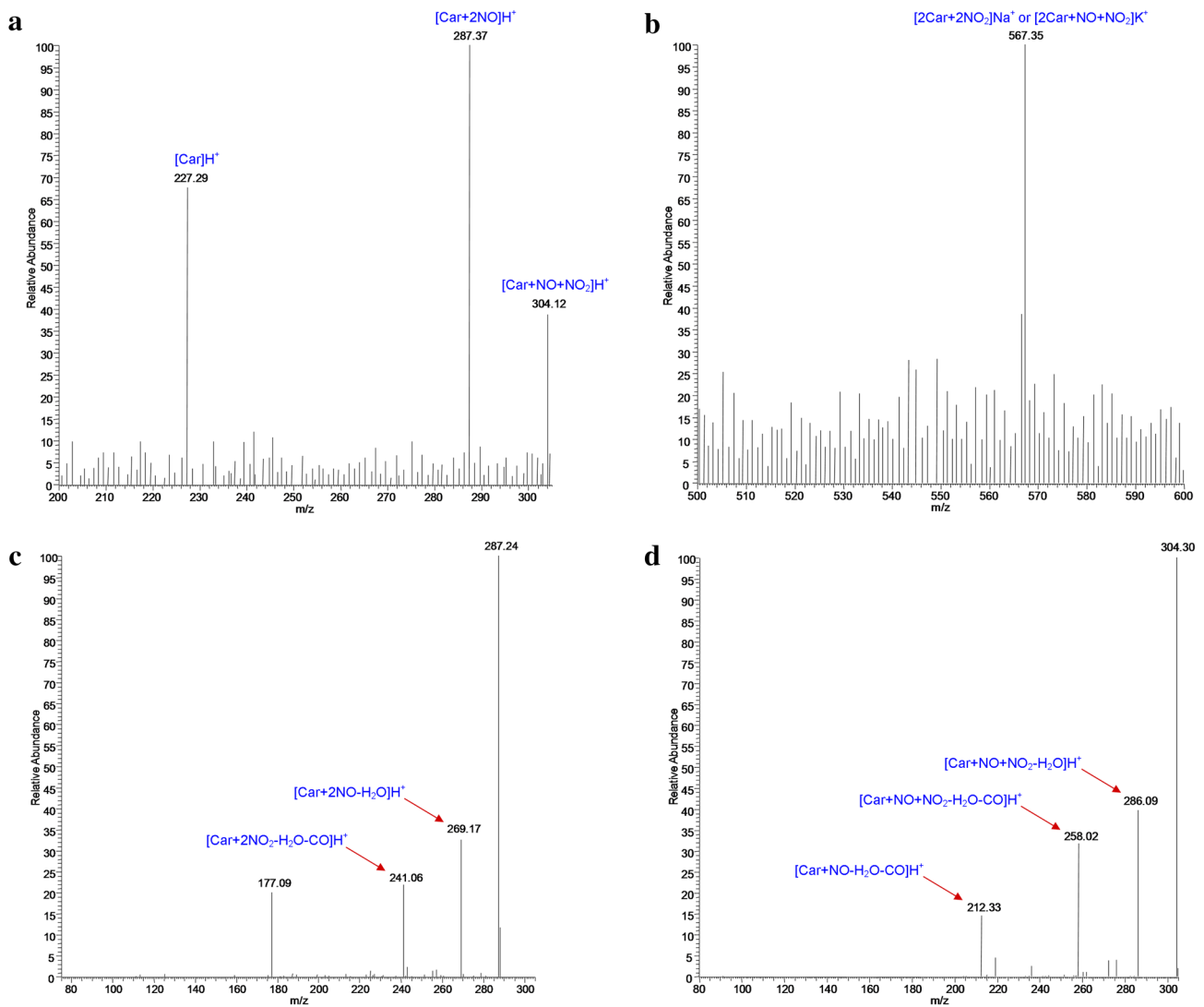
a

b

c

d

Fig. 3 ESI-MS spectra of Car (10 µM) in the presence of DEA/NO at a Car/DEA/NO ratio of 1:1 (**a, b**). CID of m/z 287 (**c**) and CID of m/z 304 (**d**)

$[Car + NO – H_2O – CO]H^+$ were obtained from CID of m/z 304 (Fig. 3d).

^{13}C-NMR spectroscopy to study the interaction mechanism of Car with NO

NMR experiments were carried out with the intent to better understand whether both constituent amino acids (β-Ala and His) of Car are involved in the interaction that occurs between Car and NO. ^{13}C-NMR spectra of Car (50 mM), DEA/NO (50 mM), and a mixture of the dipeptide and the NO-donor (molar ratio 1:1) in aqueous solution are shown in Fig. 4a–c. Table 2 shows the chemical shifts in ppm (δ) of the carbon signals for Car alone and in the presence of the NO-donor. In the presence of the NO-donor, a downfield shift of the signals was more evident for the α', β'

carbon peaks, the carbon signals of the imidazole ring of His in positions 2 and 5, and –CONH– (Table 2). In addition, the chemical shift of the carbon α' was decreased in the presence of NO-donor.

Car alters expression levels of murine macrophage activation markers

The effects of the different stimulation protocols (no treatment, LPS + IFN-γ stimulation, in the presence or absence of Car) on the cell morphology are shown in Online Resource 3. In order to determine the biological consequences regarding Car modulation of NO on macrophages, we investigated the upregulation of immune activation markers following stimulation. We observed that cells activated with LPS + IFN-γ (24 h) showed an
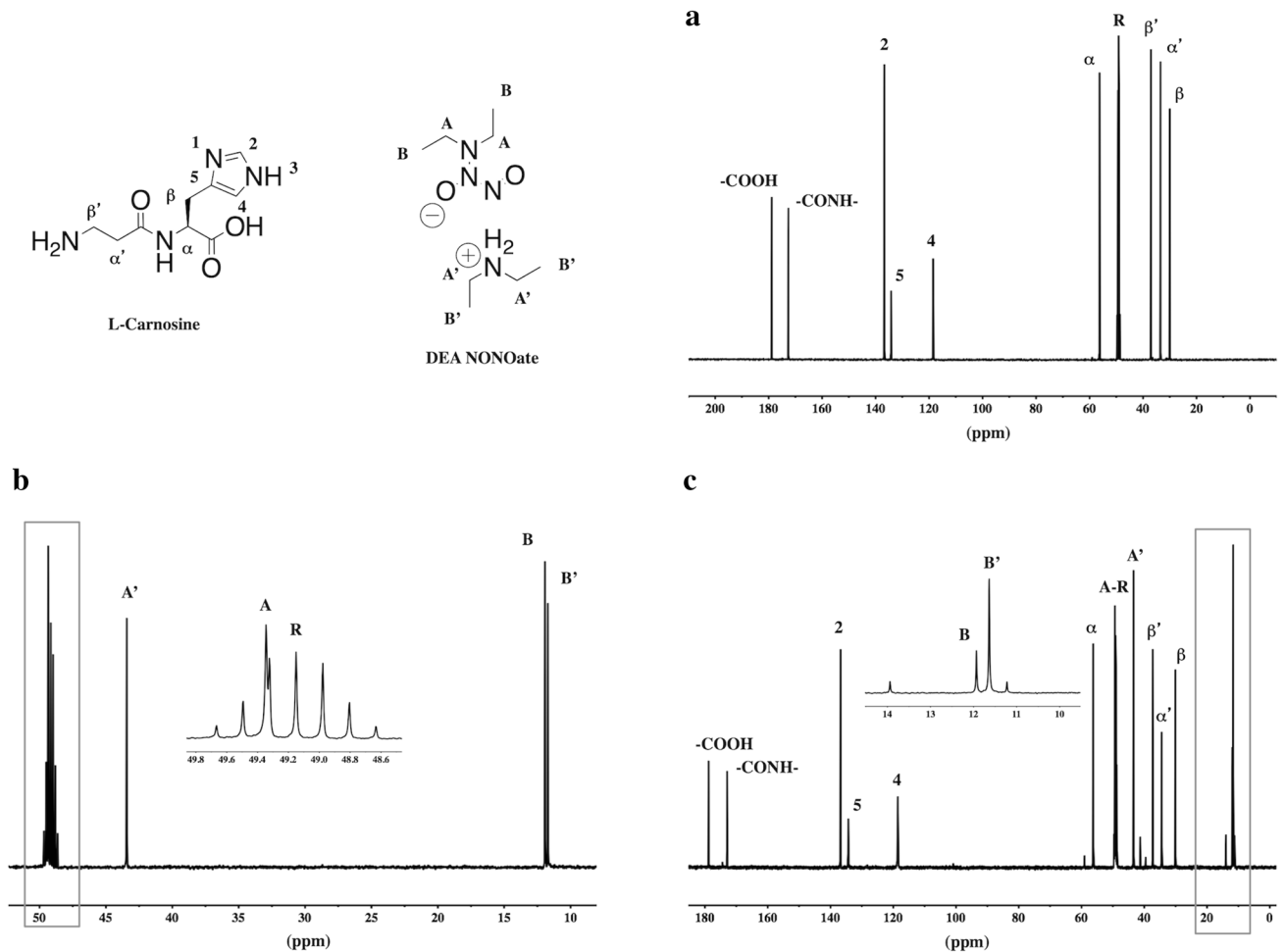
Fig. 4 ^{13}C-NMR spectra of 50 mM Car (**a**), 50 mM DEA NONOate (**b**), and a mixture of Car and NO-donor (molar ratio 1:1) (**c**) in H_2O/ CD$_3$OD (9/1 v/v). Chemical shifts of the signals are relative to CD$_3$OD (R)

Table 2 Results from 1D ^{13}C-NMR study of carnosine and nitric oxide

	–COOH	–CONH–	C2	C5	C4	Cα	Cβ'	Cα'	Cβ
Car	178.81	172.58	136.71	134.21	118.48	56.27	37.04	33.44	29.98
Car + DEA/NO	178.84	172.93	136.77	134.31	118.52	56.25	37.29	34.42	30.07

Chemical shifts of carbon signals of carnosine (Car) alone (50 mM) and in the presence of the nitric oxide donor DEA NONOate (DEA/NO) (50 mM). The chemical shifts are expressed in ppm and referred to the internal reference CD$_3$OD

increase in forward scatter measurements compared with resting cells (Online Resource 4). Preincubation with Car diminished the LPS + IFN-γ macrophage-mediated size increase. The levels of MHCII in these cells were then measured. It was found, as expected, that cell stimulation increased MHCII receptor levels. However, there was no significant difference in the amounts of MHC receptors between stimulated cells whether in the absence or the presence of Car (data not shown). The percentage of CD86+ cells was also not affected

when cells were pretreated with Car compared with cells that were stimulated with only LPS + IFN-γ (Online Resource 5). We then measured the coexpression levels of MHCII and CD206 in order to measure M1/M2 state in these cells. We found that 1-h pretreatment with Car reduced the percentages of both M1- and M2-activated cells (Fig. 5). However, preincubation of cells with Car increased the percentage of immature cells as defined by MHCII− CD206−. A significant reduction in the M2-activated subpopulation (MHCII + CD206+) was
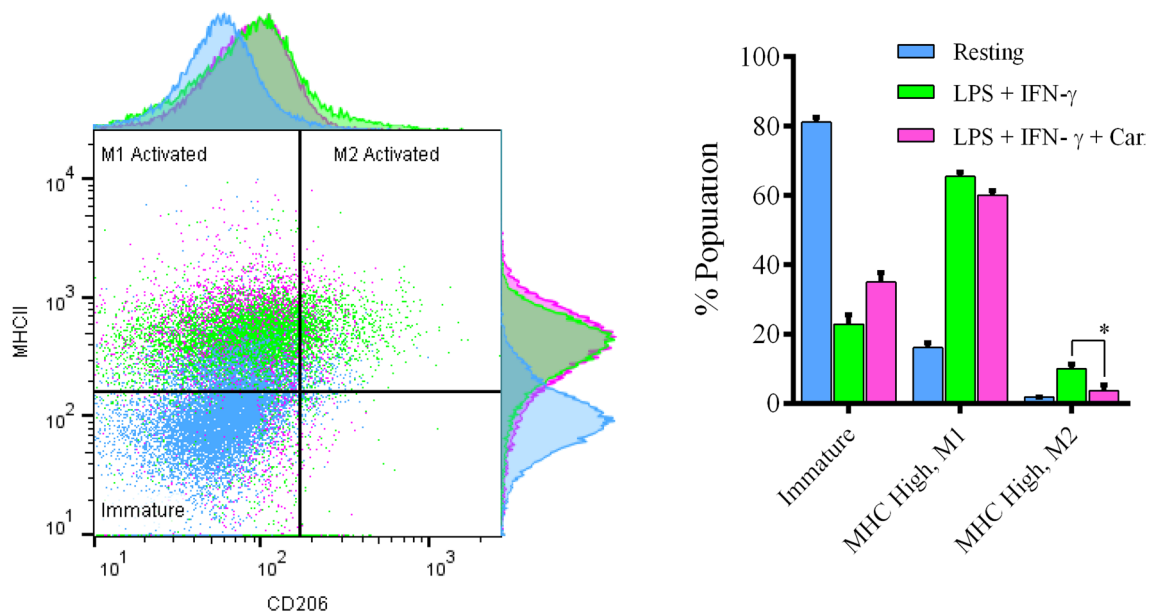
Fig. 5 M1/M2 activation. The effect of Car pretreatment (1 h) on LPS + IFN-γ-stimulated macrophages (24 h) was analyzed using flow cytometry. M1-activated (MHCII+, CD206−) and M2-activated (MHCII+, CD206+) subpopulations were measured. Quantification of M1/M2 subpopulations was performed in triplicate. *Vertical bars* represent mean percent population ± standard deviation. Significant comparisons between each group are indicated by *lines*. *Significantly different from LPS + IFN-γ ($p < 0.05$)

also observed (9.9% with LPS + IFN-γ compared to 3.4% with Car pretreatment).

Pretreatment with Car significantly reduces IL-6 secretion by stimulated murine macrophages

The analysis of cytokines in cell supernatants indicated a strong upregulation of several cytokines induced by LPS + IFN-γ treatment (24 h) in both the presence and the absence of Car pretreatment (1 h) compared with resting (untreated) cells. These cytokines include IL-1β, IL-2, IL-4, IL-5, IL-6, IL-12, and TNF-α (Fig. 6). Interestingly, the levels of KC expression were markedly reduced in stimulated cells in the absence or presence of Car (Fig. 6j). The concentrations of cytokines in the supernatants obtained from stimulated cells pretreated with Car were slightly different than those of cells without Car. Only IL-6 (Fig. 6e) showed a statistically significant reduction in concentration ($p < 0.05$) when compared with the non-Car-pretreated cells.

Discussion

Results reported in the present study indicate that (a) Car (β-Ala-His), an endogenous dipeptide that is naturally present in several mammalian tissues [1], caused an apparent suppression of total NO production by cultured murine RAW 264.7 macrophages stimulated by LPS + IFN-γ; (b)

this effect was specific to Car and was not observed in the presence of its constituent amino acids β-Ala and His; (c) the dose-dependent decrease in the NO formation induced by Car in stimulated macrophages was accompanied by a drastic intracellular increase in its low toxic endproduct, nitrite; (d) Car modulation of NO was also accompanied by the modulation of macrophage activation markers and the secretion of IL-6 cytokine.

In the last two decades, interest in Car, as well as in other naturally occurring compounds, has continuously grown either with the intent to better clarify their pathophysiological roles [21] or because of their potential pharmacological applications in different pathological states [30]. In most instances, the beneficial effects of Car treatment were related to its generally ascribed antioxidant activity [31], which involves a capacity to decrease both ROS and RNS in different experimental models [32, 33]. In agreement with these and other studies, our experiments with cultured murine RAW 264.7 macrophages, using ME-LIF to detect the stable fluorescent NO adduct in cell lysates [27, 34], confirmed that Car decreases the NO concentration in stimulated cells in a dose-dependent manner (Fig. 1 and Online Resource 1). This effect has previously been ascribed to the inhibition of the iNOS overexpression in other immune cells, since iNOS is responsible for most of the NO generation following stimulation with LPS + IFN-γ [33]. In the present study, we measured NO and nitrite in the same cell lysates and observed that the inhibition of NO induced by Car was not accompanied by a decrease
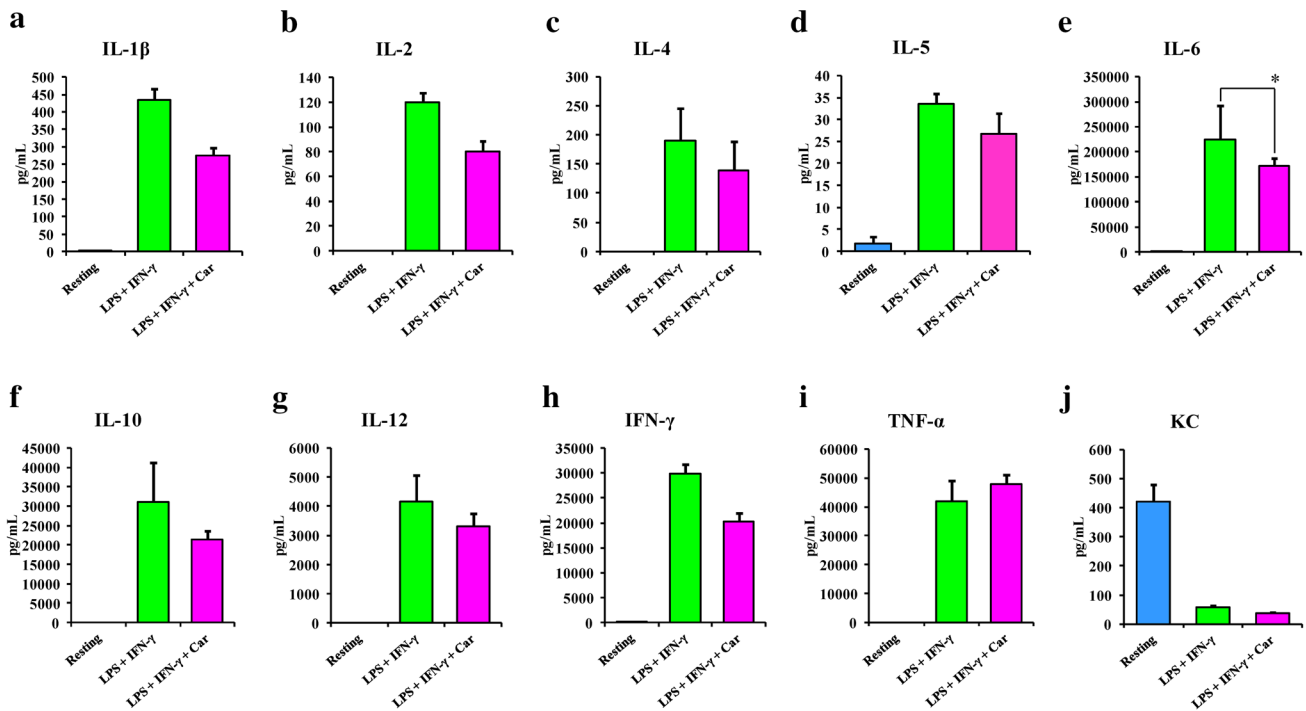
Fig. 6 Cytokine secretion. Supernatants from resting macrophages and macrophages stimulated with LPS + IFN-γ (24 h) with or without Car pretreatment (1 h) were analyzed using a multiplex cytokine assay. Each treatment was analyzed in duplicate, and each cytokine determination was performed in duplicate wells. *Vertical bars* represent mean ± standard deviation pictograms of biological duplicates. Significant comparisons between each group are indicated by *lines*. *Significantly different from LPS + IFN-γ ($p < 0.05$)

in the total nitrite. Rather surprisingly, we found that Car dose-dependently increased the concentration of intracellular nitrite (Fig. 2 and Online Resource 2). This result was confirmed by further experiments in which we found that this effect was obtained only with Car. The two amino acids making up the Car peptide, β-Ala and His, did not generate significant changes in nitrite concentration. By assuming that all the nitrite that we found in both the cell lysates (intracellular) and medium (extracellular) are derived from the decomposition of macrophage-produced NO, and by referring the extracellular NO to the number of cells, it was possible to calculate that the sum of NO + intracellular nitrite + extracellular nitrite in stimulated macrophages was approximately 12.39 nmol/10^6 cells and that of cells pretreated with Car and then stimulated was approximately 12.31 nmol/10^6 cells (Table 3). Therefore, Car did not affect the total NO production induced by cell stimulation.

In a parallel set of experiments, we found a dramatic overexpression of protein iNOS induced by LPS + IFN-γ that was not significantly counteracted by pretreating cells for 1 h with Car. These results were further verified and confirmed by the Arg/Cit ratio (Table 1), a well-established indirect indicator of iNOS activity [35, 36]. Thus, Car does not either negatively affect iNOS protein expression or inhibit iNOS activity.

Table 3 Nitric oxide and nitrite production in murine RAW 264.7 macrophages

Cell treatment	Nitric oxide[a] (intracellular)	Nitrite[a] (intracellular)	Nitrite[a] (extracellular)	Total[a]
Resting	0.07 ± 0.02	0.70 ± 0.15	0.65 ± 0.16	1.42
LPS + IFN-γ	2.82 ± 0.32	4.31 ± 0.36	5.26 ± 0.42	12.39
LPS + IFN-γ + Car	0.10 ± 0.01	8.80 ± 0.75	3.41 ± 0.60	12.31

Sum of intracellular nitric oxide + intracellular and extracellular nitrite in resting macrophages, in macrophages stimulated with LPS + IFN-γ (24 h), and in macrophages stimulated with LPS + IFN-γ (24 h) supplemented with 20 mM carnosine (Car) (1-h pretreatment). Values are the means of five different experiments ± SD

[a] nmol/10^6 cells

Hence, if both NO and total nitrite (intracellular and extracellular) had not been measured in these studies, the results of the cellular experiments might have given rise to two limitative and erroneous interpretations of the results: (1) that Car caused a decrease in NO production (if considering NO only); and (2) that Car increased NO production, while indirectly evaluating NO through nitrite determination only. Instead, the concomitant determination of both NO and its stable endproduct, nitrite, showed evidence that Car, under the present experimental conditions, did not modify the total NO production (NO + total nitrite) of stimulated macrophages. This finding is in contrast to previous reports of an increase in NO formation induced by Car in endothelial cells (when NO production was evaluated by measuring nitrite only) [37] or a decrease in NO formation (when NO production was measured by assaying only NO) [20].

To investigate the interaction between Car and NO produced by macrophages, we carried out ESI-MS and ^{13}C-NMR experiments. The existence of Car–NO adducts previously proposed by Nicoletti [20] and Fleisher-Berkovich [33] is consistent with our ESI-MS and ^{13}C-NMR analyses. Our experimental data suggest that Car can combine with two molecules of NO, giving a 1:2 adduct (m/z 287), and/ or a molecule of NO and one of NO_2^- (m/z 304) (Fig. 3a). It is important to note that an adduct with an m/z = 567 is very probably formed by two molecules of Car and two of nitrite (Fig. 3b). If the formation of this adduct also occurs in the stimulated macrophages, it might explain the apparent unequal distribution of intracellular and extracellular nitrite in the presence of Car. Indeed, as recently described by Fresta et al. [38], Car is readily taken up by RAW 264.7 macrophages in cell culture, and cell stimulation with LPS + IFN-γ leads to pronounced Car uptake and an unequal distribution of intracellular (higher due to the increased uptake) and extracellular (lower because part of Car is now inside the cell) concentrations of Car compared to that of unstimulated cells. Intracellular nitrite might then be trapped as the 2 Car–2 nitrite adduct (Fig. 3b) (more concentrated in the intracellular environment) as well as Car–NO–NO_2 (Fig. 3a). These compounds, under the strong acidic conditions of the Griess assay, might decompose, releasing nitrite and leading to its apparent higher increase within the macrophages. Interestingly, the fragmentation of m/z 287 and 304 produced a loss of water and carbon monoxide (m/z 241 and 256, respectively) (Fig. 3c, d) but not a loss of NO and/or NO_2^-, which suggests that donor adduct formation does not occur at the carboxyl group of Car.

^{13}C-NMR analysis supported the interaction of Car with NO in solution. It can be seen that, after having added the NO-donor to a solution of Car, the observed chemical shifts for the dipeptide changed (Fig. 4c; Table 2). Interestingly,

a downfield shift of the signals of carbon α′ and β′, the two carbons in position 5 and 2 of the imidazole ring of the His moiety, and the carbon of the amide bond was more evident than for the other carbons of Car. These results suggest that the interaction of NO/NO_2^- with Car in solution could occur with the -NH_2 of the β-Ala, the -CONH-, and the N in position 1 of the imidazole ring. ^{13}C-NMR and ESI-MS studies demonstrated that the ability of Car to interact with NO/NO_2^- depended on β-Ala and the imidazole ring of His. These observations were in agreement with the finding that Car derivatives [20] and/or the amino acid β-Ala and His alone did not generate any adduct with NO.

The flow cytometry experiments showed that Car pretreatment has an effect on LPS + IFN-γ-mediated activation of macrophages. Car did not exhibit global inhibition of activation markers, as demonstrated by a lack of change in upregulation of MHCII. Conversely, an effect was seen in the levels of CD206, which suggests that the M2 population is diminished (Fig. 5). The decrease in the CD206 marker suggests that Car might be able to alter the M1/ M2 macrophage ratio, thus enabling the modulation of macrophage-mediated inflammation processes. This is in agreement with previous studies in which antioxidants were found to alter M2 polarization through ROS modulation [26]. When cells were preincubated with Car and stimulated with LPS + IFN-γ, a lower amount of IL-6 in supernatants was detected compared to that in cells stimulated in the absence of Car (Fig. 6e). Il-6 has recently been described as an important cytokine for alternate macrophage activation [39]. This observation could provide an explanation for the reduction in M2 polarization indicated by the flow cytometric results, although further in vitro and in vivo studies with models of inflammation are certainly needed. This provides a rationale to investigate the role of Car in modulating IL-6 signaling in macrophages under conditions, such as atherosclerosis, obesity, and cancer, where alternative macrophages activation is of critical importance. Car pretreatment also decreased the production of other pro-inflammatory markers, including IL-1β, IL-2, IL-4, IL-5, IL-10, IL-12, and IFN-γ, although to a lesser extent. These results are in agreement with those obtained by Ooi et al. showing the ability of Zn-Car conjugates to inhibit inflammatory mediators production in LPS-activated RAW 264.7 cells [40]. Interestingly, TNF-α levels obtained from cells treated with LPS + IFN-γ in the presence of Car were comparable to those found in the supernatants of stimulated cells treated in the absence of Car. Nevertheless, a decreasing concentration of TNF-α was observed when cells were pretreated with the increasing concentrations (5, 10, and 20 mM) of Car (Online Resource 6), suggesting that, different from the other pro-inflammatory markers, higher concentrations of Car (>20 mM) are necessary to produce significantly lower TNF-α levels than those found

in supernatants of cells treated with LPS + IFN-γ in the absence of Car.

The results of the present study strongly suggest that Car, rather than decreasing the overall amount of NO formation, is directly interacting with NO by favoring oxidation of NO to its low toxic endproduct nitrite. Thus, it does not inhibit NO production in activated RAW 264.7 macrophages, according to preliminary data reported by Karabay et al. [41]. These results indicate an alternative mechanism for the hypothesized influence of Car on iNOS gene expression [32, 33]. In fact, it is evident that, under our experimental conditions of iNOS activation, a faster removal of NO from the cell environment (transformed by Car into nitrite) reduces the possibility of RNS formation (including peroxynitrite) [42]. This then limits oxidative damage to macromolecules with relevant beneficial effects for cell health and survival [30]. Although previous studies have indicated that Car might decrease NO production through the formation of stable Car–NO adducts [20], our results led us to hypothesize that Car somehow intervenes by accelerating the conversion of NO into nitrite via a still unknown mechanism. It may also be possible that part of the beneficial effects of Car are due to just an increase in nitrite, since it has been demonstrated that nitrite can alleviate the effects of cerebral vasospasms [43] and can attenuate ischemia–reperfusion injury in the heart and liver [43, 44]. These beneficial effects of nitrite are very relevant under hypoxic conditions, where it has been suggested that it functions as an important source of NO for vasoregulation [45].

Although further experiments are needed to determine the exact mechanism, our findings show, for the first time to the best of our knowledge, that Car (but not its constituent amino acids) caused an increase in the amount of NO converted into nitrite by directly interacting with NO, thereby strongly suggesting a novel mechanism through which Car decreases apparent NO formation in stimulated murine RAW 264.7 macrophages. It may explain in part the beneficial effects of Car in reducing cell damage due to the overproduction of ROS and RNS.

Compliance with ethical standards

Conflict of interest The authors declare that they have no conflict of interest.

Informed consent Not applicable. This is an in vitro study.

Research involving human participants and/or animals This article does not contain any studies with human participants performed by any of the authors.

References

1. Blaise GA, Gauvin D, Gangal M, Authier S (2005) Nitric oxide, cell signaling and cell death. Toxicology 208:177–192
2. Vallance P (1992) Endothelial regulation of vascular tone. Postgrad Med J 68:697–701
3. Schlossmann J, Feil R, Hofmann F (2003) Signaling through NO and cGMP-dependent protein kinases. Ann Med 35:21–27
4. Lane P, Gross SS (1999) Cell signaling by nitric oxide. Semin Nephrol 19:215–229
5. Pacher P, Beckman JS, Liaudet L (2007) Nitric oxide and peroxynitrite in health and disease. Physiol Rev 87:315–424
6. Aktan F (2004) iNOS-mediated nitric oxide production and its regulation. Life Sci 75:639–653
7. Calabrese V, Mancuso C, Calvani M, Rizzarelli E, Butterfield DA, Stella AM (2007) Nitric oxide in the central nervous system: neuroprotection versus neurotoxicity. Nat Rev Neurosci 8:766–775
8. Martinez FO, Helming L, Gordon S (2009) Alternative activation of macrophages: an immunologic functional perspective. Annu Rev Immunol 27:451–483
9. Maes M, Galecki P, Chang YS, Berk M (2011) A review on the oxidative and nitrosative stress (O&NS) pathways in major depression and their possible contribution to the (neuro)degenerative processes in that illness. Prog Neuropsychopharmacol Biol Psychiatry 35:676–692
10. Trachootham D, Lu W, Ogasawara MA, Nilsa RD, Huang P (2008) Redox regulation of cell survival. Antioxid Redox Signal 10:1343–1374
11. Schulz JB, Lindenau J, Seyfried J, Dichgans J (2000) Glutathione, oxidative stress and neurodegeneration. Eur J Biochem 267:4904–4911
12. Lopalco A, Dalwadi G, Niu S, Schowen RL, Douglas J, Stella VJ (2016) Mechanism of decarboxylation of pyruvic acid in the presence of hydrogen peroxide. J Pharm Sci 105:705–713
13. Lopalco A, Douglas J, Denora N, Stella VJ (2016) Determination of pK a and hydration constants for a series of α-keto-carboxylic acids using nuclear magnetic resonance spectrometry. J Pharm Sci 105:664–672
14. Lopalco A, Stella VJ (2016) Effect of Molecular structure on the relative hydrogen peroxide scavenging ability of some α-keto carboxylic acids. J Pharm Sci 105:2879–2885
15. Gariballa SE, Sinclair AJ (2000) Carnosine: physiological properties and therapeutic potential. Age Ageing 29:207–210

16. Hobart LJ, Seibel I, Yeargans GS, Seidler NW (2004) Anti-crosslinking properties of carnosine: significance of histidine. Life Sci 75:1379–1389

17. Guiotto A, Calderan A, Ruzza P, Borin G (2005) Carnosine and carnosine-related antioxidants: a review. Curr Med Chem 12:2293–2315

18. Bellia F, Vecchio G, Cuzzocrea S, Calabrese V, Rizzarelli E (2011) Neuroprotective features of carnosine in oxidative driven diseases. Mol Aspects Med 32:258–266

19. Fontana M, Pinnen F, Lucente G, Pecci L (2002) Prevention of peroxynitrite-dependent damage by carnosine and related sulphonamido pseudodipeptides. Cell Mol Life Sci 59:546–551

20. Nicoletti VG, Santoro AM, Grasso G, Vagliasindi LI, Giuffrida ML, Cuppari C, Purrello VS, Stella AM, Rizzarelli E (2007) Carnosine interaction with nitric oxide and astroglial cell protection. J Neurosci Res 85:2239–2245

21. Boldyrev AA, Aldini G, Derave W (2013) Physiology and pathophysiology of carnosine. Physiol Rev 93:1803–1845

22. Martinez FO, Gordon S (2014) The M1 and M2 paradigm of macrophage activation: time for reassessment. F1000Prime Rep 6:13

23. Mills CD, Kincaid K, Alt JM, Heilman MJ, Hill AM (2000) M-1/M-2 macrophages and the Th1/Th2 paradigm. J Immunol 164:6166–6173

24. Lee J, Ryu H, Ferrante RJ, Morris SM Jr, Ratan RR (2003) Translational control of inducible nitric oxide synthase expression by arginine can explain the arginine paradox. Proc Natl Acad Sci USA 100:4843–4848

25. Munder M (2009) Arginase: an emerging key player in the mammalian immune system. Br J Pharmacol 158:638–651

26. Zhang Y, Choksi S, Chen K, Pobezinskaya Y, Linnoila I, Liu ZG (2013) ROS play a critical role in the differentiation of alternatively activated macrophages and the occurrence of tumor-associated macrophages. Cell Res 23:898–914

27. Mainz ER, Gunasekara DB, Caruso G, Jensen DT, Hulvey MK, da Silva JAF, Metto EC, Culbertson AH, Culbertson CT, Lunte SM (2012) Monitoring intracellular nitric oxide production using microchip electrophoresis and laser-induced fluorescence detection. Anal Methods 4:414–420

28. Amorini AM, Giorlandino C, Longo S, D'Urso S, Mesoraca A, Santoro ML, Picardi M, Gullotta S, Cignini P, Lazzarino D, Lazzarino G, Tavazzi B (2012) Metabolic profile of amniotic fluid as a biochemical tool to screen for inborn errors of metabolism and fetal anomalies. Mol Cell Biochem 359:205–216

29. Förstermann U, Sessa WC (2012) Nitric oxide synthases: regulation and function. Eur Heart J 3:829–837, 837a–837d

30. Budzen S, Rymaszewska J (2013) The biological role of carnosine and its possible applications in medicine. Adv. Clin Exp Med 22:739–744

31. Cararo JH, Streck EL, Schuck PF, Ferreira Gda C (2015) Carnosine and related peptides: therapeutic potential in age-related disorders. Aging Dis 6:369–379

32. Tsai SJ, Kuo WW, Liu WH, Yin MC (2010) Antioxidative and anti-inflammatory protection from carnosine in the striatum of MPTP-treated mice. J Agric Food Chem 58:11510–11516

33. Fleisher-Berkovich S, Abramovitch-Dahan C, Ben-Shabat S, Apte R, Beit-Yannai E (2009) Inhibitory effect of carnosine and N-acetyl carnosine on LPS-induced microglial oxidative stress and inflammation. Peptides 30:1306–1312

34. Metto EC, Evans K, Barney P, Culbertson AH, Gunasekara DB, Caruso G, Hulvey MK, da Silva JAF, Lunte SM, Culbertson CT (2013) An integrated microfluidic device for monitoring changes in nitric oxide production in single T lymphocyte (Jurkat) cells. Anal Chem 85:10188–10195

35. Karkhaneh A, Ansari M, Emamgholipour S, Rafiee MH (2015) The effect of 17β-estradiol on gene expression of calcitonin gene-related peptide and some pro-inflammatory mediators in peripheral blood mononuclear cells from patients with pure menstrual migraine. Iran J Basic Med Sci 18:894–901

36. Lacza Z, Snipes JA, Zhang J, Horváth EM, Figueroa JP, Szabó C, Busija DW (2003) Mitochondrial nitric oxide synthase is not eNOS, nNOS or iNOS. Free Radic Biol Med 35:1217–1228

37. Takahashi S, Nakashima Y, Toda K (2009) Carnosine facilitates nitric oxide production in endothelial f-2 cells. Biol Pharm Bull 32:1836–1839

38. Fresta CG, Hogard ML, Caruso G, Costa EE, Lazzarino G, Lunte SM (2017) Monitoring carnosine uptake by RAW 264.7 macrophage cells using microchip electrophoresis with fluorescence detection. Anal Methods 9:402–408

39. Mauer J, Chaurasia B, Goldau J, Vogt MC, Ruud J, Nguyen KD, Theurich S, Hausen AC, Schmitz J, Brönneke HS, Estevez E, Allen TL, Mesaros A, Partridge L, Febbraio MA, Chawla A, Wunderlich FT, Brüning JC (2014) Signaling by IL-6 promotes alternative activation of macrophages to limit endotoxemia and obesity-associated resistance to insulin. Nat Immunol 15:423–430

40. Ooi TC, Chan KM, Sharif R (2016) Zinc carnosine inhibits lipopolysaccharide-induced inflammatory mediators by suppressing NF-κb activation in Raw 264.7 macrophages, independent of the MAPKs signaling pathway. Biol Trace Elem Res 172:458–464

41. Karabay AZ, Koc A, Ozkan T, Sunguroglu A, Buyukbingol Z (2010) Carnosine does not inhibit nitric oxide production in LPS-activated RAW 264.7 macrophages. Int Immunol Meet Abstr 22(Suppl 1 Pt 1):i48–i50. doi:10.1093/intimm/dxq080

42. Huie RE, Padmaja S (1993) The reaction of no with superoxide. Free Radic Res Commun 18:195–199

43. Pluta RM, Dejam A, Grimes G, Gladwin MT, Oldfield EH (2005) Nitrite infusions to prevent delayed cerebral vasospasm in a primate model of subarachnoid hemorrhage. JAMA 293:1477–1484

44. Duranski MR, Greer JJ, Dejam A, Jaganmohan S, Hogg N, Langston W, Patel RP, Yet SF, Wang X, Kevil CG, Gladwin MT, Lefer DJ (2005) Cytoprotective effects of nitrite during in vivo ischemia-reperfusion of the heart and liver. J Clin Invest 115:1232–1240

45. Donzelli S, Switzer CH, Thomas DD, Ridnour LA, Espey MG, Isenberg JS, Tocchetti CG, King SB, Lazzarino G, Miranda KM, Roberts DD, Feelisch M, Wink DA (2006) The activation of metabolites of nitric oxide synthase by metals is both redox and oxygen dependent: a new feature of nitrogen oxide signaling. Antioxid Redox Signal 8:1363–1371